STUDIES AND RESEARCHES - V.26, 2006
Graduate School in Concrete Structures – Fratelli Pesenti
Politecnico di Milano, Italy

BIAXIAL BENDING OF CONCRETE COLUMNS: AN ANALYTICAL SOLUTION

L. Cedolin[1], G. Cusatis[2], S. Eccheli, M. Roveda[3]

ABSTRACT

This paper deals with the computation of the failure envelope of rectangular R/C cross sections subjected to biaxial bending and to an axial force, at the ultimate limit state. Due to the non linearity of the constitutive laws for both steel and concrete, it is practically impossible to find the exact analytical solution. Although the problem can be solved numerically and suitable numerical algorithms are available in the literature, an analytical solution would be highly.

In this study an approximate solution is proposed in the form of a power representation (Bresler curve) of the failure envelope, whose ingredients are the ultimate bending moments along the axes of symmetry and the power exponent.

Accurate numerical simulations show that the power exponent depends on the axial force, on the reinforcement ratio and on the dimensionless cover (the ratio between the rebar cover and the length of the side of the cross section). This dependence can be computed by constraining the Bresler curve to match a particular failure point of the interaction diagram, for which the neutral axis is parallel to one of the diagonals of the cross section. The computation of the coordinates of this point is straightforward, if one observes that - in the plane of the dimensionless force and moment terms – this point corresponds to the uniaxial bending of an equivalent square cross section along a diagonal. Based on this observation, explicit analytical expressions are derived for the interaction diagram in this direction, which, together with the interaction diagrams in the principal directions, provide the data for the calculation of the power exponent of the Bresler curve. Finally, numerical simulations are performed in order to check the accuracy of the approximate analytical formulation.

[1] Professor, Dept. of Structural Engineering, Politecnico di Milano, Milan, Italy.
[2] Assistant Professor, Dept. of Civil and Environmental Engineering, Johnsson Engineering Center, Rensselaer Polytechnic Institute, Troy (NY), USA.
[3] MS Structural Engineers, Milan, Italy.

1. INTRODUCTION

A reinforced concrete column may be subjected to an axial load acting eccentrically with respect to both principal axes of the cross section. The design of the column then requires the computation of the cross section's failure surface, expressed in terms of the axial load and of the components about the principal axes of the bending moment at failure. The intersections of this surface with the coordinate planes, corresponding to the interaction diagrams in the principal directions, can be calculated easily, because the bending is uniaxial. Finding an analytical solution for the intersection of the failure surface with a third plane, corresponding to the interaction diagram for a load eccentricity acting in the same plane, is exceedingly difficult because the bending is biaxial. This difficulty has led to the use of abaci, tables or expressions of the bending moment at failure based on empirical combinations of the ultimate bending moments in the principal directions.

This paper introduces a novel analytical method for the determination of the interaction diagram for a particular direction of the load eccentricity, for which the bending in dimensionless form can be studied as uniaxial. This interaction diagram, together with the ones in the principal directions, can be used to obtain by interpolation an accurate approximation of the failure surface. The original idea at the basis of this approach was outlined in a recent conference contribution [1].

2. RESISTANCE OF CROSS SECTIONS SUBJECT TO FLEXURE AND AXIAL LOAD

Let us consider a cross section subjected to flexure and axial load (Fig. 1a). Assuming that the cross section remains plane during the deformation process, we can write, for a certain position of the neutral axis,

$$\varepsilon = \varepsilon_{top} \frac{\eta}{\eta_n} \tag{1}$$

where ε is the strain at a generic point (note that shortening is assumed positive), η is the distance from the neutral axis, ε_{top} is the strain at the most compressed point of the cross section (point C in Fig. 1a), $\eta_n = b\, \varepsilon_{top}/(\varepsilon_{top} - \varepsilon_{bot})$ is the distance between point C and the neutral axis, and b is the depth of the cross section in the direction orthogonal to the neutral axis.

From the stress-strain curves of steel and concrete, shown in Fig. 2, and the strain profile defined by Eq. 1 it is possible to compute the stress $\sigma_{s,i}$ in the rebars and σ_c in the compressed concrete. By integrating the stress over the cross section and assuming that each rebar can be regarded as a steel area concentrated in one point, we obtain the internal axial force and the internal bending moments (Eqs. 2a-c).

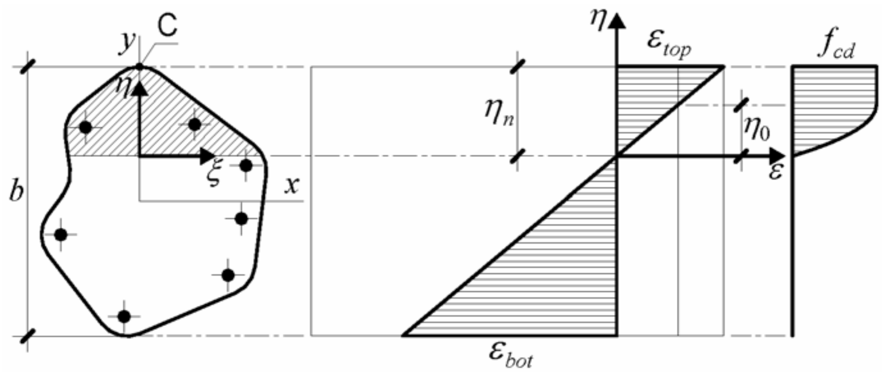

Fig. 1. a) Generic reinforced concrete cross section, b) strain profile, and c) stress profiles.

$$
\begin{aligned}
N &= \int_{\Omega} \sigma_c \, d\Omega + \sum_i A_{s,i} \, \sigma_{s,i} \\
M_x &= \int_{\Omega} \sigma_c \, y \, d\Omega + \sum_i A_{s,i} \, \sigma_{s,i} \, y_{s,i} \\
M_y &= \int_{\Omega} \sigma_c \, x \, d\Omega + \sum_i A_{s,i} \, \sigma_{s,i} \, x_{s,i}
\end{aligned}
\tag{2}
$$

When the strain profile expressed by Eq. 1 corresponds to a limit state, Eqs. 2a-c give the ultimate resistances N_{Ru}, M_{Rux}, M_{Ruy} of the cross section. According to Eurocode 2 [2] and to the Italian building code for reinforced concrete structures [3] we consider two limit states: 1) crushing of concrete defined by $\varepsilon_{top} = \varepsilon_{cu}$, and 2) steel failure defined by $\varepsilon_{s,max} = \varepsilon_{su}$. The ultimate strain ε_{cu} is reduced to ε_{c0} when the cross section is uniformly compressed, ε_{c0} being the strain at peak stress of the stress-strain curve of concrete (Fig. 2b).

The failure envelope $f(N, M_x, M_y) = 0$ for a generic cross section can be determined point by point by assuming different positions of the neutral axis and calculating the integrals in Eqs. 2a-c numerically.

In this study, for the case of a rectangular cross section of sides a and b (Fig. 5), we seek a power approximation [4] of the failure envelope in the form

$$\left[\frac{\mu_x}{\mu_{Rux}(v)}\right]^{\alpha(v)} + \left[\frac{\mu_y}{\mu_{Ruy}(v)}\right]^{\alpha(v)} = 1 \tag{3}$$

in which $\mu_x = M_x/(a\, b^2 f_{cd})$, $\mu_y = M_y/(a^2\, b f_{cd})$, $v = N/(a\, b f_{cd})$ are the dimensionless bending moments and axial force [5] at failure, f_{cd} is the design strength of concrete and $\mu_{Rux}(v)$, $\mu_{Ruy}(v)$ are the dimensionless ultimate moments for bending along the axes of symmetry x and y. We will show that, by using the dimensionless variables μ_x, μ_y and v, it is possible to analyze a rectangular cross section through the response of an equivalent square cross section.

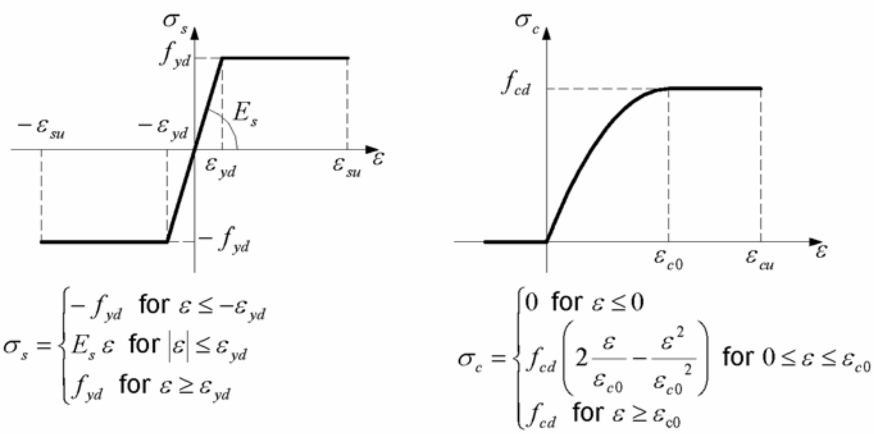

Fig. 2. Uniaxial stress-strain curves for steel and concrete.

3. EXACT SOLUTIONS FOR SQUARE CROSS SECTIONS

Let us consider a square cross section reinforced with a rebar at each corner (Fig. 3). We can compute the exact analytical expression of the interaction diagrams in parametric form for bending along the axes of symmetry x and y (parallel to the sides) and along the two diagonals. We distinguish between three different types of ultimate strain profiles, shown in Fig. 3 for bending along the axes of symmetry and in Fig. 4 for bending along the diagonals. Type 1 strain profile is characterized by steel failure, Type 2 by concrete crushing and Type 3 by concrete crushing with reduced ultimate strain. A smooth transition between these three different failure modes can be obtained by rotating the straight line defining the strain profile about the points P_1, P_2, P_3 defined in Figs. 3 and 4.

In the following we will compute separately the contributions of concrete and steel to the resistance of the cross section. In other words we write $N_{Ru} = N_{Ru,c} + N_{Ru,s}$ where $N_{Ru,c}$, $N_{Ru,s}$ are the integral over Ω and the sum over i, respectively, in Eq. 2a. We do the same for M_{Rux} and M_{Ruy}, and, for sake of simplicity, in the following we will drop the subscript "*Ru*".

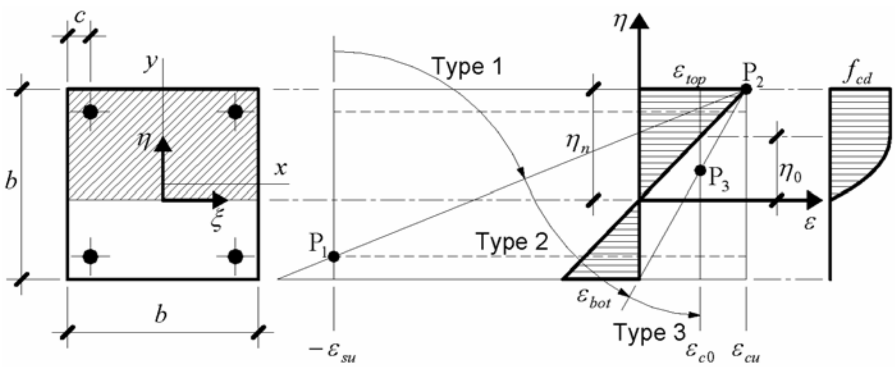

Fig. 3. Flexure along axes of symmetry parallel to the sides of a square cross section.

3.1 Flexure along axes of symmetry parallel to the sides

Fig. 3 shows a cross section subject to bending along the y-axis. Three types of strain profiles previously considered can be defined through Eqs. 4 and 5

$$\varepsilon_{top} = \begin{cases} \dfrac{\varepsilon_{su}\,\eta_n}{b - c - \eta_n} & \text{Type 1} \\ \varepsilon_{cu} & \text{Type 2} \\ \dfrac{\varepsilon_{c0}\,\varepsilon_{cu}\,\eta_n}{\varepsilon_{cu}\,\eta_n - b\left(\varepsilon_{cu} - \varepsilon_{c0}\right)} & \text{Type 3} \end{cases} \tag{4}$$

and

$$\varepsilon \equiv \varepsilon_{top}\frac{\eta}{\eta_n}; \qquad \eta_0 = \eta_n \frac{\varepsilon_{c0}}{\varepsilon_{top}} \tag{5a-b}$$

in which ε_{top} is the concrete strain in the most compressed face of the section and η_n is the distance of this face from the neutral axis. The variable η is the distance of a generic point of the cross section from the neutral axis. For $\eta = \eta_0$ the strain is equal to ε_{c0}.

For Type 1 failure we can distinguish three different sub-cases: 1A, 1B and 1C. If $\varepsilon_{top} \le 0$ (case 1A) the neutral axis is outside the cross section ($\eta_n \le 0$) and concrete is everywhere under tension. According to stress-strain law adopted for concrete we have

$$N_c^{1A} = 0; \qquad M_{cy}^{1A} = 0 \tag{6a-b}$$

If $0 < \varepsilon_{top} \le \varepsilon_{c0}$ ($0 < \eta_n \le (b - c)\, \varepsilon_{c0}/(\varepsilon_{su} + \varepsilon_{c0})$, case 1B) only the parabolic portion of the constitutive law plays a role and we get

$$N_c^{1B} = b\,\eta_n\, f_{cd} \left(\frac{\varepsilon_{top}}{\varepsilon_{c0}} - \frac{\varepsilon_{top}{}^2}{3\,\varepsilon_{c0}{}^2} \right) \tag{7}$$

The eccentricity η_c^{1B} of N_c^{1B} with respect to the neutral axis is

$$\eta_c^{1B} = \frac{b\, f_{cd}\, \eta_n^2}{N_c^{1B}} \left(\frac{2\varepsilon_{top}}{3\varepsilon_{c0}} - \frac{\varepsilon_{top}{}^2}{4\varepsilon_{c0}{}^2} \right) \tag{8}$$

By using Eqs. 7, 8 we can then calculate the bending moment as

$$M_{cy}^{1B} = N_c^{1B} \left(b/2 - \eta_n + \eta_c^{1B} \right) \tag{9}$$

If $\varepsilon_{c0} < \varepsilon_{top} \le \varepsilon_{cu}$ ($(b - c)\, \varepsilon_{c0}/(\varepsilon_{su} + \varepsilon_{c0}) < \eta_n \le (b - c)\, \varepsilon_{cu}/(\varepsilon_{su} + \varepsilon_{cu})$, case 1C) both the parabolic portion and the plateau of the stress-strain curve enter in the calculations and we have

$$N_c^{1C} = b\, f_{cd} \left(\eta_n - \frac{\eta_0}{3} \right); \qquad \eta_c^{1C} = \frac{b\, f_{cd}}{N_c^{1C}} \left(\frac{\eta_n{}^2}{2} - \frac{\eta_0{}^2}{12} \right) \tag{10a-b}$$

The bending moment M_{cy}^{1C} can be calculated similarly to M_{cy}^{1B} (see Eq. 9).

For Type 2 failure ($(b - c)\, \varepsilon_{cu}/(\varepsilon_{su} + \varepsilon_{cu}) < \eta_n \le b$) the behavior of the cross section is governed by the same equations as in the case 1C

$$N_c^2 = N_c^{1C}; \qquad M_{cy}^2 = M_{cy}^{1C} \tag{11a-b}$$

For Type 3 failure the neutral axis lies outside the cross section ($\eta_n > b$) and strains and stresses are always positive (compression) throughout the cross section. In this case we have

$$N_c^3 = b\, f_{cd} \left(\frac{(\eta_n - b)^3}{3\eta_0^{\ 2}} - \frac{(\eta_n - b)^2}{\eta_0} + \eta_n - \frac{\eta_0}{3} \right) \tag{12}$$

$$\eta_c^3 = \frac{b\, f_{cd}}{N_c^3} \left(\frac{(\eta_n - b)^4}{4\eta_0^{\ 2}} - \frac{2}{3}\frac{(\eta_n - b)^3}{\eta_0} + \frac{\eta_n^{\ 2}}{2} - \frac{\eta_0^{\ 2}}{12} \right) \tag{13}$$

Once again the bending moment M_{cy}^3 is given by an equation similar to Eq. 9. Because of the symmetry of the cross section, we always have $M_{cx} = 0$.

Obviously the previous equations govern also the behavior of the cross section subjected to bending along the x-axis. In this case we have $M_{cy} = 0$ and in the previous equations x substitutes y.

3.2 Flexure along the diagonals

Let us now consider the bending of a square cross section along one of the diagonals (Fig. 4). We can still use Eqs. 4 and 5 if we substitute b by $b\sqrt{2}$ and c by $c\sqrt{2}$.

With the same procedure as before we can calculate the counterpart of the ultimate axial force and of the bending moments about the x and y axes, associated with concrete stress distribution only. Because of the symmetry, the bending moment about x is equal to the bending moment about y

$$M_{cx} = M_{cy} \tag{14a-b}$$

For this reason, in the following we report the expression of the bending moments without the subscripts x or y.

For Type 1 failure with $\eta_n \leq 0$ (case 1A) we have

$$N_c^{1A} = 0; \qquad M_c^{1A} = 0 \tag{15a-b}$$

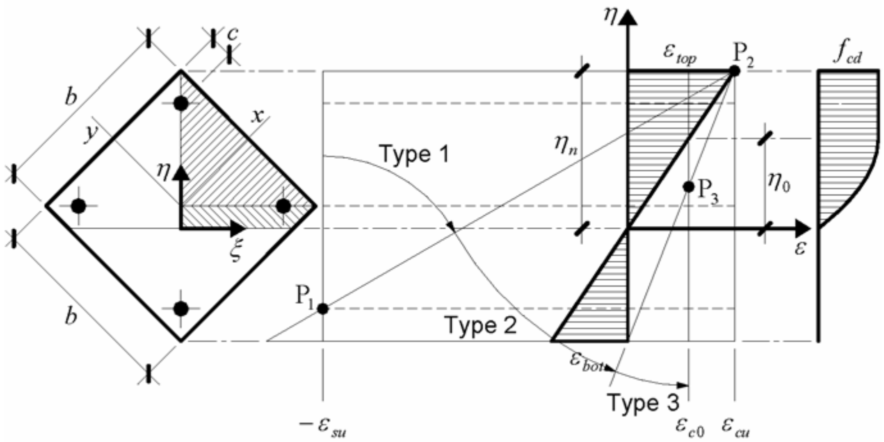

Fig. 4. Flexure along the diagonals of a square cross section.

Type 1 failure with $0 < \eta_n \le \sqrt{2}(b-c)\varepsilon_{c0}/(\varepsilon_{c0}+\varepsilon_{su})$ is again labeled as case 1B. Since $\varepsilon_{c0} << \varepsilon_{su}$ we have that $\eta_n < b\sqrt{2}/2$ and then the compressed zone has a triangular shape. Denoting as usual with η_c^{1B} the eccentricity of the resultant with respect to the neutral axis, we obtain

$$N_c^{1B} = f_{cd}\left(\frac{2}{3}\frac{\eta_n^{\,3}}{\eta_0} - \frac{\eta_n^{\,4}}{6\eta_0^{\,2}}\right); \qquad \eta_c^{1B} = \frac{f_{cd}}{N_c}\left(\frac{\eta_n^{\,4}}{3\eta_0} - \frac{\eta_n^{\,5}}{10\eta_0^{\,2}}\right) \tag{16a-b}$$

$$M_c^{1B} = N_c^{1B}\left(b/2 - \eta_n\sqrt{2}/2 + \eta_c^{1B}\sqrt{2}/2\right) \tag{17}$$

For Type 1 failure with $\eta_n \le \sqrt{2}(b-c)\varepsilon_{cu}/(\varepsilon_{cu}+\varepsilon_{su})$ and $\eta_n > \sqrt{2}(b-c)\varepsilon_{c0}/(\varepsilon_{c0}+\varepsilon_{su})$ (case 1C) the compressed zone is still a triangle because $\varepsilon_{cu} << \varepsilon_{su}$ and then $\eta_n < b\sqrt{2}/2$. We obtain

$$N_c^{1C} = f_{cd}\left(\eta_n^{\,2} - \frac{2}{3}\eta_n\eta_0 + \frac{\eta_0^{\,2}}{6}\right); \qquad \eta_c^{1C} = \frac{f_{cd}}{N_c^{1C}}\left(\frac{\eta_n^{\,3}}{3} - \frac{\eta_n\eta_0^{\,2}}{6} + \frac{\eta_0^{\,3}}{15}\right) \tag{18a-b}$$

The bending moment M_c^{1C} is calculated similarly to M_c^{1B} through Eq. 17.

Eqs. 18a-b hold also for Type 2 failure mode as long as $\eta_n \le b\sqrt{2}/2$. We label this case as 2A:

$$N_c^{2A} = N_c^{1C}; \qquad M_c^{2A} = M_c^{1C} \tag{19a-b}$$

For Type 2 failure with $b\sqrt{2}/2 < \eta_n \le b\sqrt{2}$ (case 2B) the compressed zone is no longer a triangle, but the sum of a triangle and a trapezoid. The resultants of the stress distributions and their eccentricities with respect to the neutral axis associated with the triangle ($N_{c1}^{2B}, \eta_{c1}^{2B}$) and the trapezoid ($N_{c2}^{2B}, \eta_{c2}^{2B}$) read

$$N_{c1}^{2B} = f_{cd}\left[\frac{\eta_n^{\,4}}{6\eta_0^{\,2}} - \frac{2}{3}\frac{\eta_n^{\,3}}{\eta_0} + \eta_n^{\,2}\left(1-\frac{b^2}{2\eta_0^{\,2}}\right) + \eta_n\left(\frac{\sqrt{2}}{3}\frac{b^3}{\eta_0^{\,2}} + \frac{b^2}{\eta_0} - \frac{2}{3}\eta_0\right) - \frac{b^4}{8\eta_0^{\,2}} + \right.$$
$$\left. -\frac{\sqrt{2}}{3}\frac{b^3}{\eta_0} + \frac{\eta_0^{\,2}}{6}\right] \tag{20}$$

$$N_{c2}^{2B} = f_{cd}\left(\sqrt{2}\,\eta_n - b\right)^2\left[\frac{\eta_n^{\,2}}{12\eta_0^{\,2}} - \frac{\eta_n}{\eta_0}\left(\frac{\sqrt{2}}{4}\frac{b}{\eta_0} + \frac{1}{3}\right) + \frac{5}{24}\frac{b^2}{\eta_0^{\,2}} + \frac{2\sqrt{2}}{3}\frac{b}{\eta_0}\right] \tag{21}$$

$$\eta_{c1}^{2B} = \frac{f_{cd}}{N_{c1}^{2B}}\left[\frac{\eta_n^{\,5}}{10\eta_0^{\,2}} - \frac{\eta_n^{\,4}}{3\eta_0} + \eta_n^{\,3}\left(\frac{1}{3} - \frac{b^2}{2\eta_0^{\,2}}\right) + \eta_n^{\,2}\left(\frac{\sqrt{2}}{2}\frac{b^3}{\eta_0^{\,2}} + \frac{b^2}{\eta_0}\right) + \right.$$
$$\left. -\eta_n\left(\frac{9}{24}\frac{b^4}{\eta_0^{\,2}} + \frac{2\sqrt{2}}{3}\frac{b^3}{\eta_0} + \frac{\eta_0^{\,2}}{6}\right) + \frac{\sqrt{2}}{20}\frac{b^5}{\eta_0^{\,2}} + \frac{b^4}{4\eta_0} + \frac{\eta_0^{\,3}}{15}\right] \tag{22}$$

$$\eta_{c2}^{2B} = \frac{f_{cd}}{N_{c2}^{2B}}\left(\sqrt{2}\,\eta_n - b\right)^3\left[\frac{\sqrt{2}}{40}\frac{\eta_n^{\,2}}{\eta_0^{\,2}} - \frac{\eta_n}{\eta_0}\left(\frac{7}{40}\frac{b}{\eta_0} + \frac{\sqrt{2}}{12}\right) + \frac{3\sqrt{2}}{40}\frac{b^2}{\eta_0^{\,2}} + \frac{5}{12}\frac{b}{\eta_0}\right] \tag{23}$$

The total axial force is the sum of the two resultants ($N_c^{2B} = N_{c1}^{2B} + N_{c2}^{2B}$) and the bending moment about the centroid of the cross section is given by the sum of the moments of the two resultants:

$$M_c^{2B} = N_{c1}^{2B}\left(b/2 - \eta_n\sqrt{2}/2 + \eta_{c1}^{2B}\sqrt{2}/2\right) + N_{c2}^{2B}\left(b/2 - \eta_n\sqrt{2}/2 + \eta_{c2}^{2B}\sqrt{2}/2\right) \tag{24}$$

For Type 3 failure the entire cross section is compressed $\eta_n > b\sqrt{2}$. As in the previous case 2B we calculate the resultant of the stress distribution and its eccentricity with respect to the neutral axis separately for the two triangles. For the triangle on the upper part of the section Eqs. 20, 22 hold and then we have $N_{c1}^{3} = N_{c1}^{2B}$, $\eta_{c1}^{3} = \eta_{c1}^{2B}$. For the triangle in the lower part of the cross section we have

$$N_{c2}^{3} = f_{cd}\, b^{2}\left[-\frac{{\eta_n}^{2}}{2{\eta_0}^{2}} + \frac{\eta_n}{\eta_0}\left(\frac{2\sqrt{2}}{3}\frac{b}{\eta_0}+1\right) - \frac{11}{24}\frac{b^{2}}{{\eta_0}^{2}} - \frac{2\sqrt{2}}{3}\frac{b}{\eta_0}\right] \tag{25}$$

$$\eta_{c2}^{3} = \frac{f_{cd}}{N_{c2}^{3}} b^{2}\left[-\frac{{\eta_n}^{3}}{2{\eta_0}^{2}} + \frac{{\eta_n}^{2}}{\eta_0}\left(\sqrt{2}\frac{b}{\eta_0}+1\right) - y_n\left(\frac{11}{8}\frac{b^{2}}{{\eta_0}^{2}} + \frac{4\sqrt{2}}{3}\frac{b}{\eta_0}\right) + \frac{13\sqrt{2}}{40}\frac{b^{3}}{{\eta_0}^{2}} + \right.$$
$$\left. + \frac{11}{12}\frac{b^{2}}{\eta_0}\right] \tag{26}$$

Similarly to the previous case $N_c^3 = N_{c1}^3 + N_{c2}^3$ and

$$M_c^3 = N_{c1}^3\left(b/2 - \eta_n\sqrt{2}/2 + \eta_{c1}^3\sqrt{2}/2\right) + N_{c2}^3\left(b/2 - \eta_n\sqrt{2}/2 + \eta_{c2}^3\sqrt{2}/2\right) \tag{27}$$

3.3 Counterpart of the resistance associated with the rebars

The counterpart of the resistance associated with the rebars is calculated assuming that each rebar is approximated by an area concentrated in one point. The stress in each rebar is either proportional to the strain (elastic behavior) or constant (equal to the yield stress, plastic behavior). We can write

$$N_s = \sum_{i=1}^{4} A_{s,i}\,\sigma_{s,i} \tag{28}$$

$$M_{sx} = \sum_{i=1}^{4} A_{s,i}\,\sigma_{s,i}\,x_{s,i}; \qquad M_{sy} = 0 \tag{29a-b}$$

for bending along the x-axis,

$$M_{sy} = \sum_{i=1}^{4} A_{s,i}\,\sigma_{s,i}\,y_{s,i}; \qquad M_{sx} = 0 \tag{30a-b}$$

for bending along the y-axis, and

$$M_{sx} = \sum_{i=1}^{4} A_{s,i}\,\sigma_{s,i}\,x_{s,i} = M_{sy} = \sum_{i=1}^{4} A_{s,i}\,\sigma_{s,i}\,y_{s,i} \tag{31a-b}$$

for bending along the diagonals.

4. DIMENSIONLESS INTERACTION DIAGRAMS FOR RECTANGULAR CROSS SECTIONS

In the previous section the ultimate resistances N_{Ru}, M_{Rux}, M_{Ruy} of a square cross section for bending in a direction parallel either to the sides or the diagonals has been computed in parametric form, using as a parameter the distance η_n of the neutral axis from the extreme fiber of compressed concrete.

Let's consider now a rectangular cross section reinforced with four rebars (each rebar has the same area) placed at the four corners (Fig. 5) and introduce the dimensionless [5] variables ω (product of area and strength ratios), δ_x (dimensionless cover in x-direction), and δ_y (dimensionless cover in y-direction), defined in Fig. 5. As demostrated in Appendix II under the assumption that $\delta_x = \delta_y$, the ultimate resistances in dimensionless form can be calculated with reference to a square cross section with $\delta = \delta_x = \delta_y$. In the same Appendix II it is shown that flexure parallel to a diagonal in the square cross section corresponds, in the rectangular cross section, to flexure with neutral axis inclined as a diagonal and moment vector inclined perpendicularly to the other diagonal. This means that the previous study of the ultimate states of a square cross section also allows us to calculate the interaction diagrams for a rectangular cross section subjected to flexure in a direction inclined with respect to the principal axes.

There is however still the need to determine an explicit dependence of the moments M_{Rux} and M_{Ruy} on N_{Ru}. This can be done by computing in dimensionless form the exact values of particular points of the interaction diagram, and introducing approximate interpolation formulas, as shown in the following.

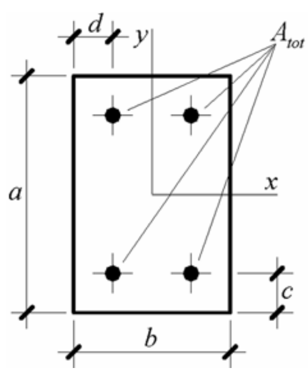

$$\omega = \frac{A_{tot}\, f_{yd}}{a b\, f_{cd}} \qquad \nu = \frac{N}{a b\, f_{cd}}$$

$$\delta_y = \frac{c}{a} \qquad \mu_y = \frac{M_y}{a^2 b\, f_{cd}}$$

$$\delta_x = \frac{d}{b} \qquad \mu_x = \frac{M_x}{a b^2\, f_{cd}}$$

Fig. 5. Rectangular cross section and dimensionless variables.

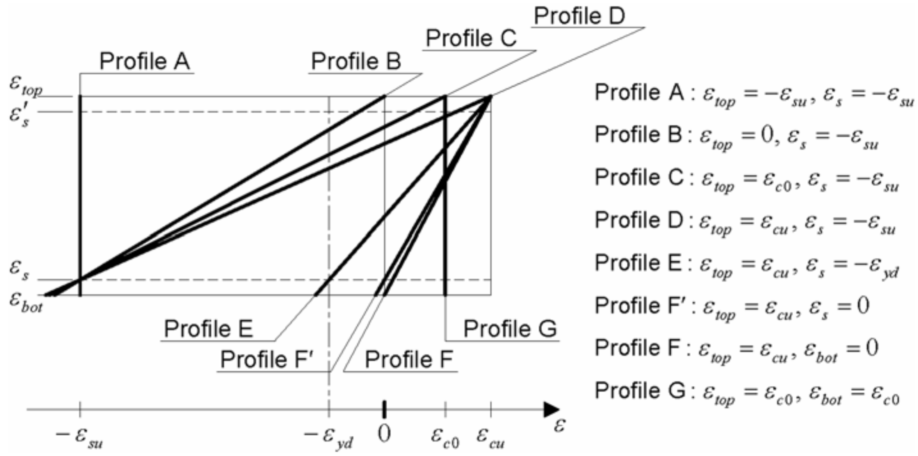

Fig. 6. Strain profiles at failure for bending along axes of symmetry.

4.1 Neutral axis parallel to the sides

We consider eight strain profiles at failure and we label them with the letters A, B, C, D, E, F′, F, and G. These strain profiles are defined by the conditions shown in Fig. 6. For each condition we can calculate the position of neutral axis as

$$\eta_n = b\left(1-\delta\right)\frac{\varepsilon_{top}}{\varepsilon_{top}-\varepsilon_s} \tag{32a-b}$$

where b, δ are b, δ_x for bending along x and a, δ_y for bending along y. In order to simplify the equations that follow, we specialize the solution for the steel Fe B 44 K (f_{yd} = 374 MPa, E_s = 206 GPa, ε_{yd} = 1.82 ‰) which is the most common steel used in Italian practice. We also input the numerical values for ε_{su}, ε_{c0} and ε_{cu} according to [3]: 1.0 %, 0.2 % and 0.35 %, respectively. Again in the following equations we will drop the subscript "*Ru*" and the subscript x or y. We get

$$\nu_{\mathrm{A}} = -\omega; \qquad \mu_{\mathrm{A}} = 0 \tag{33a-b}$$

$$\nu_{\mathrm{B}} = -\frac{\omega}{2}\left(1+5.509\frac{\delta}{1-\delta}\right); \qquad \mu_{\mathrm{B}} = \frac{\omega}{2}\left(1-5.509\frac{\delta}{1-\delta}\right)\left(\frac{1}{2}-\delta\right) \tag{34a-b}$$

$$\nu_{\mathrm{C}}=\frac{1}{9}(1-\delta)+\frac{\omega}{2}\left[1.102\left(7-\frac{6}{1-\delta}\right)-1\right];$$

$$\mu_{\mathrm{C}}=(1-\delta)\left[\frac{1}{18}-\frac{1}{144}(1-\delta)\right]+\frac{\omega}{2}\left[1.102\left(7-\frac{6}{1-\delta}\right)+1\right]\left(\frac{1}{2}-\delta\right) \tag{35a-b}$$

$$\nu_{\mathrm{D}}=\frac{17}{81}(1-\delta); \qquad \mu_{\mathrm{D}}=(1-\delta)\left[\frac{17}{162}-\frac{11}{486}(1-\delta)\right]+\omega\left(\frac{1}{2}-\delta\right) \tag{36a-b}$$

$$\nu_{\mathrm{E}}=0.533(1-\delta); \qquad \mu_{\mathrm{E}}=(1-\delta)\left[0.267-0.146(1-\delta)\right]+\omega\left(\frac{1}{2}-\delta\right) \tag{37a-b}$$

$$\nu_{\mathrm{F'}}=\frac{17}{21}(1-\delta)+\frac{\omega}{2}; \qquad \mu_{\mathrm{F'}}=(1-\delta)\left[\frac{17}{42}-\frac{33}{98}(1-\delta)\right]+\frac{\omega}{2}\left(\frac{1}{2}-\delta\right) \tag{38a-b}$$

$$\nu_{\mathrm{F}}=\frac{17}{21}+\frac{\omega}{2}(1+1.928\delta); \qquad \mu_{\mathrm{F}}=\frac{10}{147}+\frac{\omega}{2}(1-1.928\delta)\left(\frac{1}{2}-\delta\right) \tag{39a-b}$$

$$\nu_{\mathrm{G}}=1+\omega; \qquad \mu_{\mathrm{G}}=0 \tag{40a-b}$$

Note that Eqs. 34a-b have been calculated assuming that the rebars in the compressed zone remain elastic. This is true only if $\delta < 0.154$. Dimensionless rebar covers used in practice always satisfy this requirement. The Eqs. 33-40 define also the coordinates of the points A, B, …, G of the interaction diagrams for bending along the axes x and y.

For failure strain profiles between A and B we can explicitly obtain μ_{Ru} as function of ν. We have

$$\mu_{Ru}^{\mathrm{AB}}=(\nu+\omega)\left(\frac{1}{2}-\delta\right) \tag{41}$$

Between B and C, and between C and D it is not possible to obtain explicit functions for the dimensionless bending moments. Nevertheless, for usual values of ω and δ, they can be approximated accurately by straight lines:

$$\mu_{Ru}^{\mathrm{BC}}=\mu_{\mathrm{B}}+(\mu_{\mathrm{C}}-\mu_{\mathrm{B}})\frac{\nu-\nu_{\mathrm{B}}}{\nu_{\mathrm{C}}-\nu_{\mathrm{B}}}; \qquad \mu_{Ru}^{\mathrm{CD}}=\mu_{\mathrm{C}}+(\mu_{\mathrm{D}}-\mu_{\mathrm{C}})\frac{\nu-\nu_{\mathrm{C}}}{\nu_{\mathrm{D}}-\nu_{\mathrm{C}}} \tag{42a-b}$$

Between D and E, if we assume that all the rebars are no longer elastic, we can again calculate explicitly the function $\mu_{Ru}=\mu_{Ru}(\nu)$. We obtain

$$\mu_{Ru}^{\mathrm{DE}}=-\frac{297}{578}\nu^2+\frac{1}{2}\nu+\omega\left(\frac{1}{2}-\delta\right) \tag{43}$$

If $\delta > 1/9$, the rebars in the compressed zone are still elastic and Eq. 43 is not exact. However, it can be proved [6] that even in that case Eq. 43 gives a very good approximation of the exact solution.

Between E and F the curve $\mu_{Ru} = \mu_{Ru}(\nu)$ can be approximated by a parabolic function. We assume

$$\mu_{Ru}^{\mathrm{EF}} = a_0^{\mathrm{EF}}\,\nu^2 + b_0^{\mathrm{EF}}\,\nu + c_0^{\mathrm{EF}} \tag{44}$$

and we compute the coefficient a_0^{EF}, b_0^{EF}, and c_0^{EF} imposing that the points E, F′, and F satisfy Eq. 44. We obtain

$$\begin{aligned}
a_0^{\mathrm{EF}} &= \frac{\mu_{\mathrm{E}}\left(\nu_{\mathrm{F}} - \nu_{\mathrm{F}'}\right) - \mu_{\mathrm{F}'}\left(\nu_{\mathrm{F}} - \nu_{\mathrm{E}}\right) + \mu_{\mathrm{F}}\left(\nu_{\mathrm{F}'} - \nu_{\mathrm{E}}\right)}{\left(\nu_{\mathrm{F}} - \nu_{\mathrm{F}'}\right)\left(\nu_{\mathrm{F}} - \nu_{\mathrm{E}}\right)\left(\nu_{\mathrm{F}'} - \nu_{\mathrm{E}}\right)} \\
b_0^{\mathrm{EF}} &= \frac{\mu_{\mathrm{F}} - \mu_{\mathrm{E}} - a_0^{\mathrm{EF}}\left(\nu_{\mathrm{F}}{}^2 - \nu_{\mathrm{E}}{}^2\right)}{\nu_{\mathrm{F}} - \nu_{\mathrm{E}}}; \qquad c_0^{\mathrm{EF}} = \mu_{\mathrm{E}} - a_0^{\mathrm{EF}}\,\nu_{\mathrm{E}}{}^2 - b_0^{\mathrm{EF}}\,\nu_{\mathrm{E}}
\end{aligned} \tag{45a-c}$$

Finally, between F and G, where, again, an explicit solution cannot be worked out, we assume a linear approximation

$$\mu_{Ru}^{\mathrm{FG}} = \mu_{\mathrm{F}}\left(1 - \frac{\nu - \nu_{\mathrm{F}}}{\nu_{\mathrm{G}} - \nu_{\mathrm{F}}}\right) \tag{46}$$

For bending along the x-axis we have $\delta = \delta_x$, $\mu_{Rux} = \mu_{Ru}(\nu)$ e $\mu_{Ruy} = 0$ and for bending along the y-axis we have $\delta = \delta_y$, $\mu_{Ruy} = \mu_{Ru}(\nu)$ e $\mu_{Rux} = 0$.

Incidentally, we note that, for bending parallel to the sides, the foregoing expressions are valid also if the dimensionless covers are not equal. Obviously, if $\delta_x = \delta_y$ we have that $\mu_{Rux} = \mu_{Ruy}$.

It can be shown [6] that the maximum error associated with the foregoing approximated expressions is less then 2 %.

4.2 Neutral axis parallel to the diagonal

The same procedure (which uses the exact solution of an equivalent dimensionless square cross section) adopted in the previous section can be used to compute the dimensionless bending moments as function of the dimensionless axial load ($\mu_{Rux1} = \mu_{Rux1}(\nu)$, $\mu_{Ruy1} = \mu_{Ruy1}(\nu)$) for positions of the neutral axis inclined as a diagonal of the rectangle. We analyze ten strain profiles at failure labeled as A, B, C, D′, D, E, F, G′, G, and H and defined in Fig. 7.

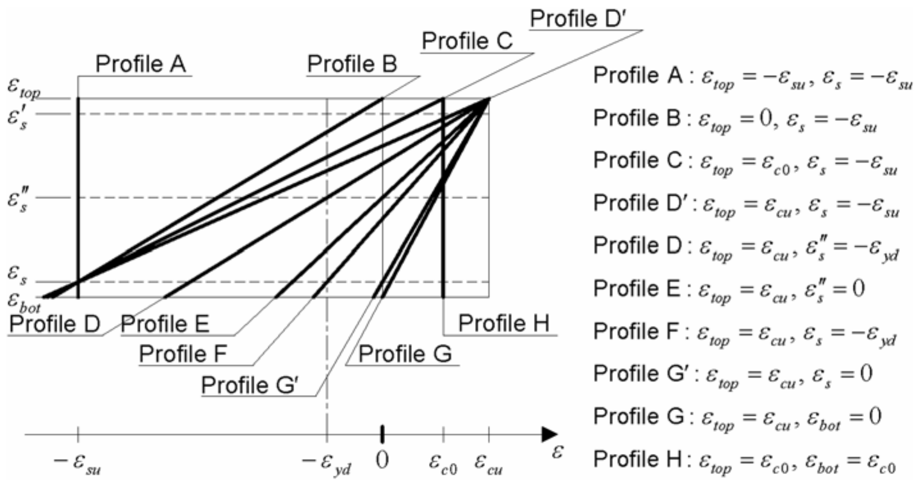

Fig. 7. Strain profiles at failure for bending along the diagonals of a rectangle.

As usual we drop, for simplicity, the subscripts "*Ru*", "*x*", and "*y*". We get

$$\nu_{\mathrm{A}} = -\omega; \qquad \mu_{\mathrm{A}} = 0 \tag{47a-b}$$

$$\nu_{\mathrm{B}} = -\frac{\omega}{4}\left(3 + 5.509\frac{\delta}{1-\delta}\right); \qquad \mu_{\mathrm{B}} = \frac{\omega}{4}\left(1 - 5.509\frac{\delta}{1-\delta}\right)\left(\frac{1}{2} - \delta\right) \tag{48a-b}$$

$$\begin{aligned} \nu_{\mathrm{C}} &= \frac{1}{36}(1-\delta)^2 + \frac{\omega}{4}\left(4.713 - \frac{6.611}{1-\delta}\right); \\ \mu_{\mathrm{C}} &= (1-\delta)^2\left[\frac{1}{72} - \frac{1}{405}(1-\delta)\right] + \frac{\omega}{4}\left(8.713 - \frac{6.611}{1-\delta}\right)\left(\frac{1}{2} - \delta\right) \end{aligned} \tag{49a-b}$$

$$\nu_{\mathrm{D'}} = \frac{22}{243}(1-\delta)^2 - \frac{\omega}{2}; \qquad \mu_{\mathrm{D'}} = (1-\delta)^2\left(\frac{11}{243} - 0.013(1-\delta)\right) + \frac{\omega}{2}\left(\frac{1}{2} - \delta\right) \tag{50a-b}$$

$$\nu_{\mathrm{D}} = 0.146 - \frac{\omega}{2}; \qquad \mu_{\mathrm{D}} = 0.046 + \frac{\omega}{2}\left(\frac{1}{2} - \delta\right) \tag{51a-b}$$

$$\nu_{\mathrm{E}} = 0.337; \qquad \mu_{\mathrm{E}} = 0.073 + \frac{\omega}{2}\left(\frac{1}{2} - \delta\right) \tag{52a-b}$$

$$\nu_{\mathrm{F}} = \frac{-0.554\delta^4 + 0.293\delta^3 + 1.999\delta^2 - 2.006\delta + 0.559}{(1-\delta)^2} + \frac{\omega}{2}\left(1.928 - \frac{1.464}{1-\delta}\right);$$

$$\mu_{\mathrm{F}} = \frac{-0.215\delta^5 + 0.228\delta^4 + 0.276\delta^3 - 0.194\delta^2 - 0.113\delta + 0.076}{(1-\delta)^2} + \frac{\omega}{2}\left(\frac{1}{2} - \delta\right) \tag{53a-b}$$

$$\nu_{\mathrm{G'}} = \frac{-1.278\delta^4 + 2.196\delta^3 + 0.644\delta^2 - 2.325\delta + 0.891}{(1-\delta)^2} + \frac{\omega}{4}\left(4.857 - \frac{1.928}{1-\delta}\right);$$

$$\mu_{\mathrm{G'}} = \frac{-0.752\delta^5 + 1.811\delta^4 - 1.177\delta^3 + 0.044\delta^2 + 0.070\delta + 0.030}{(1-\delta)^2} + \frac{\omega}{4}\left(\frac{1}{2} - \delta\right) \tag{54a-b}$$

$$\nu_{\mathrm{G}} = 0.891 + \frac{\omega}{4}\left[1 + 1.928(1+\delta)\right]; \qquad \mu_{\mathrm{G}} = 0.030 + \frac{\omega}{4}(1 - 1.928\delta)\left(\frac{1}{2} - \delta\right) \tag{55a-b}$$

$$\nu_{\mathrm{H}} = 1 + \omega; \qquad \mu_{\mathrm{H}} = 0 \tag{56a-b}$$

The points A, B, …, H of the failure envelope can be then connected by polynomial functions. Between A and B we have

$$\mu_{Ru1}^{\mathrm{AB}} = (\nu + \omega)\left(\frac{1}{2} - \delta\right) \tag{57}$$

which is exact if $\delta < 0.154$.

We connect with straight lines the points B and C, D and E, and G and H:

$$\mu_{Ru1}^{\mathrm{BC}} = \mu_{\mathrm{B}} + (\mu_{\mathrm{C}} - \mu_{\mathrm{B}})\frac{\nu - \nu_{\mathrm{B}}}{\nu_{\mathrm{C}} - \nu_{\mathrm{B}}}; \quad \mu_{Ru1}^{\mathrm{DE}} = \mu_{\mathrm{D}} + (\mu_{\mathrm{E}} - \mu_{\mathrm{D}})\frac{\nu - \nu_{\mathrm{D}}}{\nu_{\mathrm{E}} - \nu_{\mathrm{D}}};$$

$$\mu_{Ru1}^{\mathrm{GH}} = \mu_{\mathrm{G}}\left(1 - \frac{\nu - \nu_{\mathrm{G}}}{\nu_{\mathrm{H}} - \nu_{\mathrm{G}}}\right) \tag{58a-c}$$

The interaction diagram between points C and D, E and F, and F and G can be approximated by parabolic functions. We identify the coefficients of the parabolas by using, for each interval one extra point which is D′ for CD, D for EF, and G′ for FG. We obtain

$$\mu_{Ru1}^{\mathrm{CD}} = a_1^{\mathrm{CD}}\,\nu^2 + b_1^{\mathrm{CD}}\,\nu + c_1^{\mathrm{CD}} \tag{59}$$

$$a_1^{\mathrm{CD}} = \frac{\mu_{\mathrm{C}}\left(v_{\mathrm{D}} - v_{\mathrm{D}'}\right) - \mu_{\mathrm{D}'}\left(v_{\mathrm{D}} - v_{\mathrm{C}}\right) + \mu_{\mathrm{D}}\left(v_{\mathrm{D}'} - v_{\mathrm{C}}\right)}{\left(v_{\mathrm{D}} - v_{\mathrm{D}'}\right)\left(v_{\mathrm{D}} - v_{\mathrm{C}}\right)\left(v_{\mathrm{D}'} - v_{\mathrm{C}}\right)}$$

$$b_1^{\mathrm{CD}} = \frac{\mu_{\mathrm{D}} - \mu_{\mathrm{C}} - a_1^{\mathrm{CD}}\left({v_{\mathrm{D}}}^2 - {v_{\mathrm{C}}}^2\right)}{v_{\mathrm{D}} - v_{\mathrm{C}}}; \qquad c_1^{\mathrm{CD}} = \mu_{\mathrm{C}} - a_1^{\mathrm{CD}}\, {v_{\mathrm{C}}}^2 - b_1^{\mathrm{CD}}\, v_{\mathrm{C}} \tag{60a-c}$$

$$\mu_{Ru1}^{\mathrm{EF}} = a_1^{\mathrm{EF}}\, v^2 + b_1^{\mathrm{EF}}\, v + c_1^{\mathrm{EF}} \tag{61}$$

$$a_1^{\mathrm{EF}} = \frac{\mu_{\mathrm{D}}\left(v_{\mathrm{F}} - v_{\mathrm{E}}\right) - \mu_{\mathrm{E}}\left(v_{\mathrm{F}} - v_{\mathrm{D}}\right) + \mu_{\mathrm{F}}\left(v_{\mathrm{E}} - v_{\mathrm{D}}\right)}{\left(v_{\mathrm{F}} - v_{\mathrm{E}}\right)\left(v_{\mathrm{F}} - v_{\mathrm{D}}\right)\left(v_{\mathrm{E}} - v_{\mathrm{D}}\right)}$$

$$b_1^{\mathrm{EF}} = \frac{\mu_{\mathrm{F}} - \mu_{\mathrm{D}} - a_1^{\mathrm{EF}}\left({v_{\mathrm{F}}}^2 - {v_{\mathrm{D}}}^2\right)}{v_{\mathrm{F}} - v_{\mathrm{D}}}; \qquad c_1^{\mathrm{EF}} = \mu_{\mathrm{D}} - a_1^{\mathrm{EF}}\, {v_{\mathrm{D}}}^2 - b_1^{\mathrm{EF}}\, v_{\mathrm{D}} \tag{62a-c}$$

$$\mu_{Ru1}^{\mathrm{FG}} = a_1^{\mathrm{FG}}\, v^2 + b_1^{\mathrm{FG}}\, v + c_1^{\mathrm{FG}} \tag{63}$$

$$a_1^{\mathrm{FG}} = \frac{\mu_{\mathrm{F}}\left(v_{\mathrm{G}} - v_{\mathrm{G}'}\right) - \mu_{\mathrm{G}'}\left(v_{\mathrm{G}} - v_{\mathrm{F}}\right) + \mu_{\mathrm{G}}\left(v_{\mathrm{G}'} - v_{\mathrm{F}}\right)}{\left(v_{\mathrm{G}} - v_{\mathrm{G}'}\right)\left(v_{\mathrm{G}} - v_{\mathrm{F}}\right)\left(v_{\mathrm{G}'} - v_{\mathrm{F}}\right)}$$

$$b_1^{\mathrm{FG}} = \frac{\mu_{\mathrm{G}} - \mu_{\mathrm{F}} - a_1^{\mathrm{FG}}\left({v_{\mathrm{G}}}^2 - {v_{\mathrm{F}}}^2\right)}{v_{\mathrm{G}} - v_{\mathrm{F}}}; \qquad c_1^{\mathrm{FG}} = \mu_{\mathrm{F}} - a_1^{\mathrm{FG}}\, {v_{\mathrm{F}}}^2 - b_1^{\mathrm{FG}}\, v_{\mathrm{F}} \tag{64a-c}$$

It can be shown [6] that the maximum error associated with the foregoing approximated formulas is less than 2 %.

5. APPROXIMATED FAILURE ENVELOPE FOR BIAXIAL BENDING

In the previous section we have derived an approximated analytical description of the interaction diagrams between moments and axial load for flexure along the two coordinate planes and normal to the diagonals. This means that we can calculate with great accuracy three points of the dimensionless failure envelope for a certain given dimensionless axial load v. The first point $(\mu_{Rux}(v), 0)$ is associated with flexure along the x-axis of symmetry, the second point $(0, \mu_{Ruy}(v))$ is associated with flexure along the y-axis of symmetry, and the third point $(\mu_{Rux1}(v), \mu_{Ruy1}(v))$ is associated with flexure normal to the diagonal of the cross section. The first two points satisfy, by definition, the approximation of the biaxial failure envelope due to Bresler (Eq. 3). The third point can be used to evaluate the power exponent $\alpha(v)$.

If we assume that the dimensionless covers are equal $\delta_x = \delta_y = \delta$ then we can write $\mu_{Rux}(v) = \mu_{Ruy}(v) = \mu_{Ru}(v)$ and $\mu_{Rux1}(v) = \mu_{Ruy1}(v) = \mu_{Ru1}(v)$. In this case, from Eq. 3, we get

$$\alpha(v) = \frac{\ln 2}{\ln\left[\mu_{Ru}(v)/\mu_{Ru1}(v)\right]} \tag{65}$$

If $\delta_x \neq \delta_y$ (typical situation in practice) Eq. 65 can still be used but $\mu_{Ru}(v)$ and $\mu_{Ru1}(v)$ must be calculated assuming an average dimensionless cover $\overline{\delta} = (\delta_x + \delta_y)/2$.

Fig. 8 shows the comparison between the approximated and the "exact" dimensionless failure envelope of a rectangular cross section for various values of ω and v. The "exact" failure envelope has been calculated by using a very accurate numerical algorithm [6] for the calculations of the integrals in Eqs. 2a-c. We assume $\delta_x = 1/10$ e $\delta_y = 1/20$. Each quadrant is relevant to a different value of the dimensionless axial force. In the first quadrant we have $v = 0.0$, in the second $v = 0.3$, in the third $v = 0.7$, and in the fourth $v = 1.0$. For each value of v we consider two different values of ω 0.2 and 1.0.

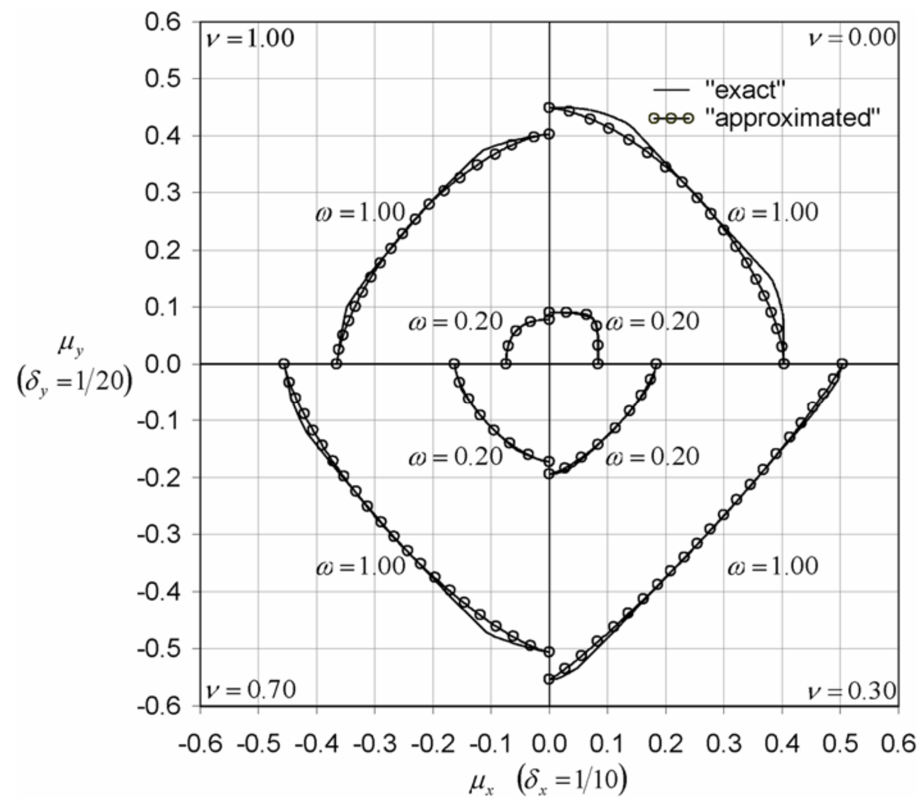

Fig. 8. Dimensionless failure envelope for a rectangular cross section.

The agreement between the approximated solution and the "exact" one appears to be very good. For higher percentages of steel, the Bresler curve deviates most from the exact curve for small inclinations of the loading plane with respect to the principal directions. This is due to the assumed steel distribution in the cross section (rebar concentrated in the corners), which makes the contribution of the rebar less sensitive to small deviations of the bending direction from the principal directions.

The same type of analysis has been developed using the constitutive laws and methodology prescribed by the ACI code [7].

6. CONCLUSIONS

An analytical solution for the failure envelope of rectangular cross sections has been formulated on the basis of a property which establishes a correspondence with an equivalent square cross section of unit side. Very accurate analytical expressions have been derived in dimensionless form for the interaction diagrams of a rectangular cross section for eccentricities of the axial load both in the direction of the axes of symmetry and that of the diagonals. Using these diagrams, it is possible to calculate with a simple formula, for a given axial load, the power exponent of an analytical expression which describes with great accuracy the failure envelope for a general bending direction. The power exponent is a function of the dimensionless axial load, of the mechanical reinforcement ratio and of the dimensionless cover, showing that the approximate constant values proposed earlier in the literature represent only crude approximations.

APPENDIX I – REFERENCES

[1] L. CEDOLIN, G. CUSATIS, S. ECCHELI, M. ROVEDA, *On the failure envelope of reinforced concrete cross sections subjected to biaxial bending and axial load: an analytical solution*, 2nd international FIB Congress, Naples, Italy, June 5-8, 2006

[2] Eurocode 2, *Design of concrete structures*, 2003.

[3] Italian Building Code for reinforced concrete structures (In Italian), D.M. 9/1/96, *Norme tecniche per il calcolo, l'esecuzione ed il collaudo delle strutture in cemento armato, normale e precompresso e per le strutture metalliche* (pubblicato sul supplemento ordinario alla Gazzetta Ufficiale della Repubblica Italiana n. 29 del 5 febbraio 1996).

[4] B. BRESLER, *Design Criteria for Reinforced Concrete Columns Under Axial Load and Biaxial Bending*, Journal ACI, 1960, pp. 481-490.
[5] F. BONTEMPI, *On the computation of the failure envelopes for reinforced concrete cross sections subjected to biaxial bending* (In Italian), Studi e ricerche n. 13 della Scuola di specializzazione in C.A. del Politecnico di Milano,1992.
[6] S. ECCHELI, M. ROVEDA, *Computer code for the analysis of reinforced concrete cross sections by using non-linear constitutive laws* (In Italian), Politecnico di Milano, Milano, Italy, 2003.
[7] L. CEDOLIN, G. CUSATIS, S. ECCHELI, M. ROVEDA, *Capacity of rectangular cross sections under biaxially eccentric loads*, submitted for publication, ACI Journal, 2006.

APPENDIX II - CORRESPONDENCE OF FAILURE CONDITIONS FOR SQUARE AND RECTANGULAR CROSS SECTIONS

Consider (Fig. 9) a square cross section of side b and a rectangular cross section of sides a, b with the only limitation that the covers d and c satisfy the condition $d/b = c/a = \delta$. This ensures that, in the case of rectangle, the rebars are situated on the diagonals.

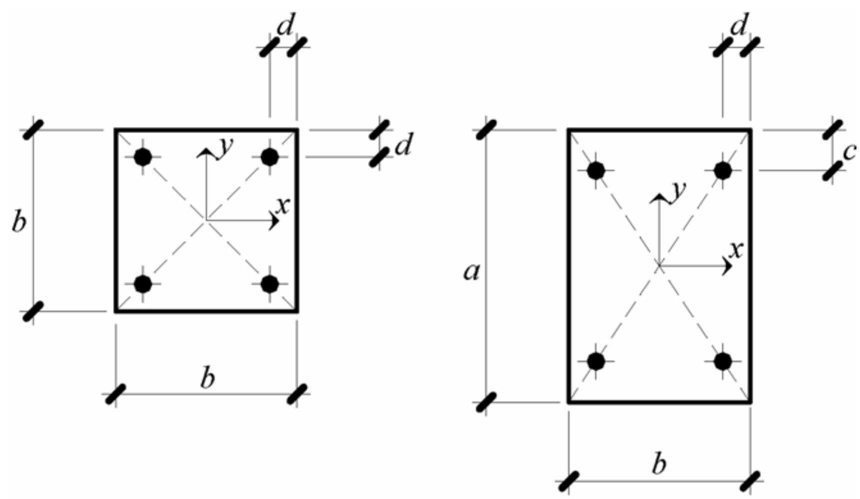

Fig. 9. Square cross section and rectangular cross section.

We want to show that from the knowledge, for the square cross section, of a failure condition (N_{Ru}, M_{Rux}, M_{Ruy}) corresponding to a given position of the neutral axis, it is possible to deduce a corresponding failure condition for the rectangular cross section. The proof is independent of the types of nonlinear constitutive relations adopted for the materials, expressed as

$$\sigma_c(\xi) = f_{cd}\, g(\varepsilon); \qquad \sigma_s = f_{yd}\, h(\varepsilon)$$

in which f_{cd}, f_{yd} are reference strength values for concrete and steel respectively, and $g(\varepsilon)$ and $h(\varepsilon)$ are dimensionless functions of strain.

The position of the neutral axis will be assigned through the distance $s = \rho\, b$ of its intercepts with side b (Fig. 10) and the inclination θ with respect to the horizontal. Let be ε^* the maximum compressive strain (positive) which caracterized the failure condition considered ($\varepsilon^* = \varepsilon_{cu}$ for concrete crushing, $\varepsilon^* < \varepsilon_{cu}$ for concrete crushing with reduced ultimate strain or for steel failure).

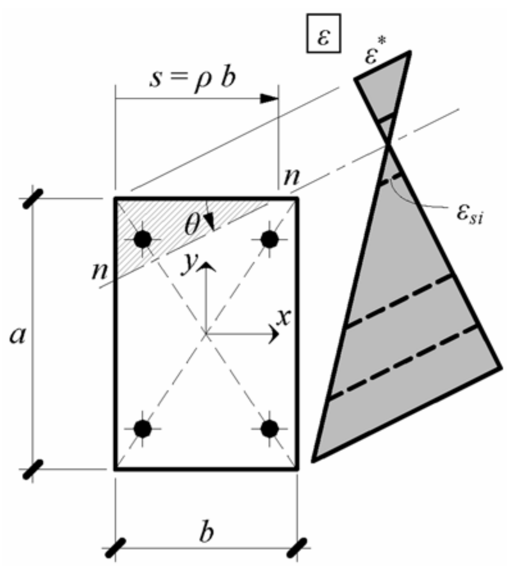

Fig. 10. Position of the neutral axis and strain distribution.

Neutral axis parallel to the sides

Let us consider (Fig. 11) flexure along the x-axis, for which the symmetrical reinforcement implies a neutral axis parallel to the other side ($\theta = \pi/2$). If u is the distance of a generic fiber from the neutral axis, its strain is given by $\varepsilon(u) = \varepsilon^* \, u/s$, and, introducing the dimensionless distance $\xi = u/s$, one obtains $\varepsilon(\xi) = \varepsilon^* \, \xi$.

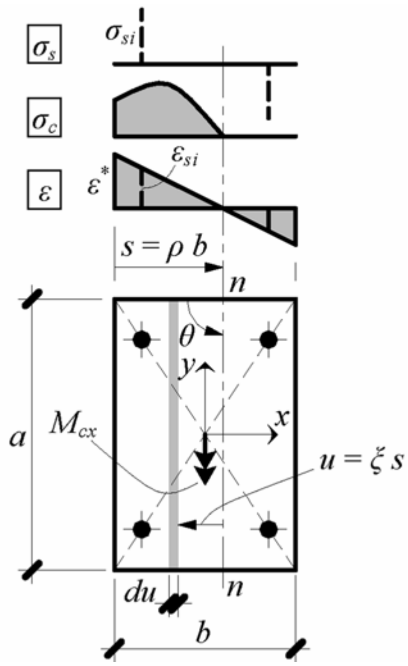

Fig. 11. Flexure along the x-axis.

Contribution from concrete

The material in a strip of width $du = s\, d\xi$ located at the dimensionless distance $\xi = u/s$ experiences the stress

$$\sigma_c(\xi) = f_{cd}\, g(\varepsilon^* \xi) = f_{cd}\, g^*(\xi)$$

The resultant of the normal stress in concrete is

$$N_c = a\int_0^s \sigma_c(u)\,du = a\int_0^1 \sigma_c(\xi)\,s\,d\xi = a\,s\,f_{cd}\int_0^1 g^*(\xi)\,d\xi = a\,b\,f_{cd}\,\rho\int_0^1 g^*(\xi)\,d\xi$$

and their moments about the centroid are $M_{cy} = 0$ and

$$M_{cx} = a\int_0^s \sigma_c(u)\left(u - s + \frac{b}{2}\right)du = a\,s^2\int_0^1 \sigma_c(\xi)\left(\xi - 1 + \frac{1}{2\rho}\right)d\xi =$$
$$= a\,b^2\,f_{cd}\,\rho^2\int_0^1 g^*(\xi)\left(\xi - 1 + \frac{1}{2\rho}\right)d\xi$$

Introducing the notation

$$G_1(\varepsilon^*,\rho) = \rho\int_0^1 g^*(\xi)\,d\xi$$
$$G_2(\varepsilon^*,\rho) = \rho^2\int_0^1 g^*(\xi)\left(\xi - 1 + \frac{1}{2\rho}\right)d\xi$$

we can put the result in the form

$$N_c(\varepsilon^*,\rho) = a\,b\,f_{cd}\,G_1(\varepsilon^*,\rho)$$
$$M_{cx}(\varepsilon^*,\rho) = a\,b^2\,f_{cd}\,G_2(\varepsilon^*,\rho)$$

which means that the dimensionless quantities

$$\nu_c = \frac{N_c}{a\,b\,f_{cd}} = G_1(\varepsilon^*,\rho)$$
$$\mu_{cx} = \frac{M_{cx}}{a\,b^2\,f_{cd}} = G_2(\varepsilon^*,\rho)$$

are independent of the ratio a/b of the sides for a given relative position ρ of the neutral axis, and consequently can be calculated with reference to a square of unit side.

Contribution from rebars

For each of the four rebars (Fig. 11) we have

$$\varepsilon_{si} = \frac{u_i}{s}\varepsilon^* = \xi_i\,\varepsilon^*$$

$$\sigma_{si} = f_{yd}\,h(\varepsilon^*\xi_i) = f_{yd}\,h^*(\xi_i)$$

$$N_s = \sum_{i=1}^{4}\sigma_{si}\,A_{si} = A_{tot}\,f_{yd}\,\frac{1}{4}\sum_{i=1}^{4}h^*(\xi_i) = A_{tot}\,f_{yd}\,H_1(\varepsilon^*,\rho)$$

$$M_{sx} = \sum_{i=1}^{4}\sigma_{si}\,A_{si}\left(u_i - s + \frac{b}{2}\right) = A_{tot}\,f_{yd}\,b\,\rho\frac{1}{4}\sum_{i=1}^{4}h^*(\xi_i)\left(\xi_i - 1 + \frac{1}{2\rho}\right) =$$

$$= A_{tot}\,f_{yd}\,b\,H_2(\varepsilon^*,\rho)$$

Using the same definition of dimensionless quantities we have

$$\nu_s = \frac{N_s}{a\,b\,f_{cd}} = \frac{A_{tot}}{a\,b}\frac{f_{yd}}{f_{cd}}H_1(\varepsilon^*,\rho)$$

$$\mu_{sx} = \frac{M_{sx}}{a\,b^2\,f_{cd}} = \frac{A_{tot}}{a\,b}\frac{f_{yd}}{f_{cd}}H_2(\varepsilon^*,\rho)$$

in which again H_1 and H_2 can be calculated with reference to a square of unit side. Introducing the mechanical reinforcement ratio

$$\omega = \frac{A_{tot}}{a\,b}\frac{f_{yd}}{f_{cd}}$$

the contribution from the rebars can put in the form

$$\nu_s = \omega\,H_1(\varepsilon^*,\rho)$$

$$\mu_{sx} = \omega\,H_2(\varepsilon^*,\rho)$$

Combined contribution

By summing the contributions of concrete and rebars, we can write

$$\nu = \nu_c + \nu_s = G_1(\varepsilon^*,\rho) + \omega\,H_1(\varepsilon^*,\rho)$$

$$\mu_x = \mu_{cx} + \mu_{sx} = G_2(\varepsilon^*,\rho) + \omega\,H_2(\varepsilon^*,\rho)$$

and note that, once obtained for a square cross section having the same reinforcement ratio, the dimensionless quantities are the same for rectangular ones.

The result may seem obvious, but the reason of this detailed demonstration is that it can be extended to bending in a direction not parallel to the sides, as we will see in the next section.

Neutral axis parallel to the diagonals

Let's consider now (Fig. 12) a particular case of biaxial bending in which the neutral axis is parallel to a diagonal ($\theta = \arctan(a/b)$).

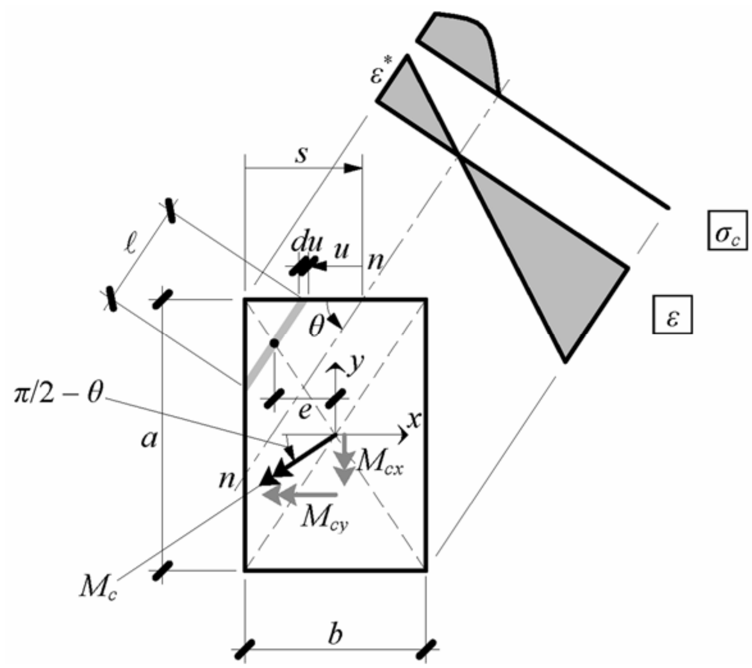

Fig. 12. Flexure along a diagonal: contribution from concrete.

Contribution from concrete

The material belonging to a strip parallel to the neutral axis experiences a strain

$$\varepsilon(u) = \varepsilon^* \frac{u}{s} = \varepsilon^* \xi$$

in which u is defined by the interception with the top side of the cross section. The corresponding stress is

$$\sigma(u) = f_{cd}\, g(\varepsilon^* \xi) = f_{cd}\, g^*(\xi) = \sigma(\xi)$$

Considering that each strip has a width (normal to the direction of the neutral axis) given by

$$du \sin\theta = s\, d\xi \sin\theta$$

and a length ℓ given by

$$\ell(u) = \ell(0)\frac{s-u}{s} = \frac{s}{\cos\theta}\left(1-\xi\right)$$

the resultant of the normal stress becomes

$$\begin{aligned} N_{cd} &= \int_0^s \sigma_c(u)\,\ell(u)\,du \sin\theta = \int_0^1 \sigma_c(\xi)\frac{s}{\cos\theta}\left(1-\xi\right) s\, d\xi \sin\theta = \\ &= s^2 \tan\theta\, f_{cd} \int_0^1 g^*(\xi)\left(1-\xi\right) d\xi \end{aligned} \qquad (**)$$

By substituting $s = \rho\, b$, $\tan\theta = a/b$, we obtain

$$N_{cd} = a\, b\, f_{cd}\, \rho^2 \int_0^1 g^*(\xi)\left(1-\xi\right) d\xi = a\, b\, f_{cd}\, G_3(\varepsilon^*, \rho, \theta)$$

The moment with respect to the centroid in the x direction can be calculated observing that the resultant of the stress acting on a strip is applied to its midpoint (intercept with the diagonal), which has eccentricity

$$e(u) = u + \frac{s-u}{2} - \left(s - \frac{b}{2}\right) = \frac{1}{2}\left(u - s + b\right) = \frac{1}{2} s \left(\xi - 1 + \frac{1}{\rho}\right)$$

and consequently

$$M_{cx} = \int_0^s \sigma_c(u)\,\ell(u)\,e(u)\,du \sin\theta = s^3 \tan\theta\, f_{cd}\, \frac{1}{2}\int_0^1 g^*(\xi)\left(1-\xi\right)\left(\xi - 1 + \frac{1}{\rho}\right) d\xi \qquad (***)$$

which becomes, with the usual notation,

$$M_{cx} = a\,b^2\, f_{cd}\,\frac{1}{2}\rho^3 \int_0^1 g^*(\xi)\left(1-\xi\right)\left(\xi - 1 + \frac{1}{\rho}\right) d\xi = a\,b^2\, f_{cd}\, G_4(\varepsilon^*, \rho, \theta)$$

We then obtain in dimensionless form

$$v_c = \frac{N_c}{a\,b\,f_{cd}} = G_3(\varepsilon^*, \rho, \theta)$$

$$\mu_{cx} = \frac{M_{cx}}{a\,b^2\, f_{cd}} = G_4(\varepsilon^*, \rho, \theta)$$

and we see again that they are independent of the ratio *a*/*b* of the sides. An analogous formula holds for the moment in the *y* direction.

It is important to note that the resultants of the stresses acting on the strips parallel to a diagonal are applied to their interception with the other diagonal. The axial force N_c is then applied to a point of this diagonal, i.e. the moment vector M_c is perpendicular to it (Fig. 12). In other words, the plane of loading passes through the diagonal which intersects the neutral axis.

If the rectangle degenerates into a square, the two diagonals are perpendicular, and so the moment vector is parallel to the neutral axis.

Contribution from steel

As already stated, we consider the situation in which the rebars are situated on the diagonals (Fig. 13). This implies that the resultant of the forces in the rebars is located on the diagonal, as for the resultant of stresses in concrete.

We have

$$\varepsilon_{si} = \frac{u_i}{s}\varepsilon^* = \xi_i\, \varepsilon^*$$

The corresponding stress is

$$\sigma_{si} = f_{yd}\, h(\varepsilon^* \xi_i) = f_{yd}\, h^*(\xi_i)$$

The resultant of the forces in the rebars is

$$N_s = \sum_{i=1}^{4} \sigma_{si}\, A_{si} = A_{tot}\, f_{yd}\, \frac{1}{4} \sum_{i=1}^{4} h^*(\xi_i) = A_{tot}\, f_{yd}\, H_3(\varepsilon^*, \rho)$$

Since the distance of the rebars from the *y*-axis is

$$e_i = \pm\left(\frac{b}{2} - d\right) = \pm b\left(\frac{1}{2} - \delta\right)$$

we see that the two rebars lying on the diagonal parallel to the neutral axis (labeled 2 and 3) give opposite contributions, which cancel each other. We can then write

$$M_{sx} = \sigma_{s1} A_{s1} b\left(\frac{1}{2}-\delta\right) - \sigma_{s4} A_{s4} b\left(\frac{1}{2}-\delta\right) = b\left(\frac{1}{2}-\delta\right) f_{yd}\left[h^*(\xi_1) - h^*(\xi_4)\right]\frac{A_{tot}}{4} =$$

$$= A_{tot}\, f_{yd}\, b\frac{1}{4}\left(\frac{1}{2}-\delta\right)\left[h^*(\xi_1) - h^*(\xi_4)\right] = A_{tot}\, f_{yd}\, b\, H_4(\varepsilon^*, \rho, \theta)$$

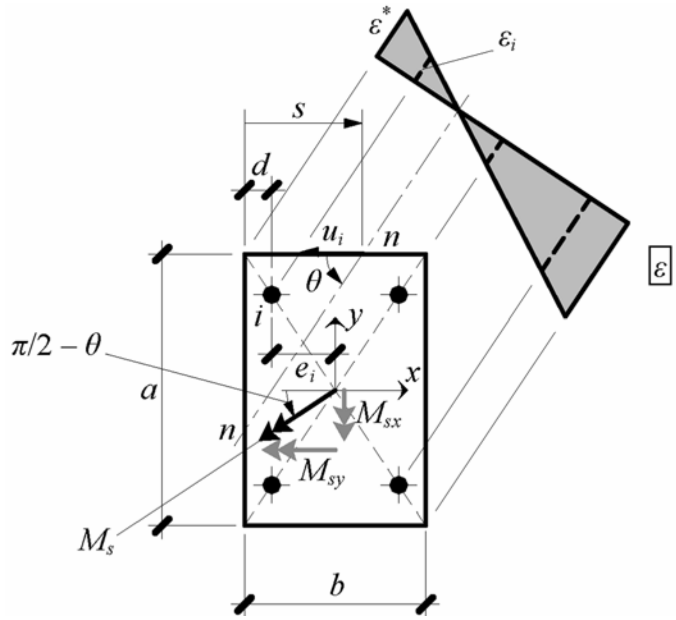

Fig. 13. Flexure along a diagonal: contribution from steel.

Introducing the dimensionless quantities,

$$\nu_s = \frac{N_s}{a\,b\,f_{cd}} = \frac{A_{tot}}{a\,b}\frac{f_{yd}}{f_{cd}} H_3(\varepsilon^*, \rho) = \omega\, H_3(\varepsilon^*, \rho, \theta)$$

$$\mu_{sx} = \frac{M_{sx}}{a\,b^2\,f_{cd}} = \frac{A_{tot}}{a\,b}\frac{f_{yd}}{f_{cd}} H_4(\varepsilon^*, \rho) = \omega\, H_4(\varepsilon^*, \rho, \theta)$$

again we recognize that they are independent of the ratio a/b of the side.
Also for the steel contribution, we note that since the resultant N_s is applied to a point of the diagonal, the resultant moment vector M_{sx} is perpendicular to the other diagonal.

Combined contributions

By summing the contributions of concrete and rebars in dimensionless form we can write

$$\nu = \nu_c + \nu_s = G_3(\varepsilon^*, \rho, \theta) + \omega H_3(\varepsilon^*, \rho, \theta)$$
$$\mu_x = \mu_{cx} + \mu_{sx} = G_4(\varepsilon^*, \rho, \theta) + \omega H_4(\varepsilon^*, \rho, \theta)$$

An analogous formula can be derived for μ_y.

We conclude then that the ultimate resistance of a rectangular cross section subjected to axial load applied along a diagonal can be studied with reference to an equivalent square cross section, for which the bending is uniaxial.

Remark

Let's consider now a generic inclination of the neutral axis, assigned through the intercepts $s = \rho\, b$ and $r = \chi\, a$ (Fig. 14).

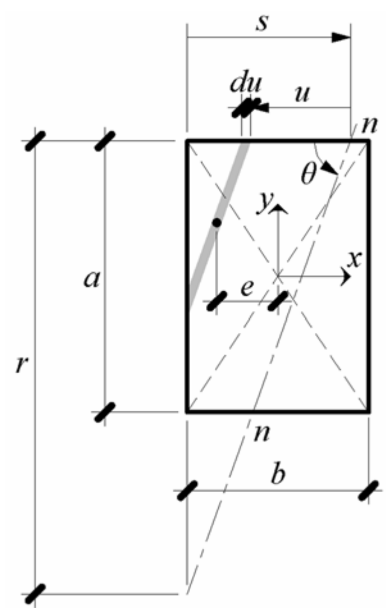

Fig. 14. Flexure in a generic direction.

For concrete, Eqs. (**) and (***) still hold. With the substitution $\tan\theta\, s^2 = r\, s = \chi\, \rho\, a\, b$ we have

$$N_c = a\,b\, f_{cd}\, \rho\, \chi\, G_3(\varepsilon^*, \rho, \chi)$$
$$M_{cx} = a\,b^2\, f_{cd}\, \rho^2\, \chi\, G_4(\varepsilon^*, \rho, \chi)$$

Analogous expressions as before hold for rebars.

We then see that, in general, any distribution of strain in a rectangular cross section can be studied through a corresponding strain distribution in a square cross section. The practical advantage of this finding, however, is restricted to the case of a neutral axis parallel to the diagonal (for which $\chi = \rho$), that has been treated in the previous section.